



Published in final edited form as:

*Free Radic Biol Med.* 2009 January 15; 46(2): 312–320. doi:10.1016/j.freeradbiomed.2008.10.045.

## Iron-Enhanced Paraquat-Mediated Dopaminergic Cell Death Due to Increased Oxidative Stress as a Consequence of Microglial Activation

Jun Peng, Fang Feng Stevenson, May Lin Oo, and Julie K. Andersen

Buck Institute for Age Research, 8001 Redwood Blvd., Novato, CA 94945

### Abstract

Environmental paraquat and neonatal iron exposure have both separately been suggested as potential risk factors for sporadic forms of Parkinson's disease (PD). In this study, we demonstrate that combined environmental exposure to these two agents results in modulations in microglial activation state. Apocynin, an NADPH oxidase inhibitor, was found to attenuate the release of superoxide from microglia stimulated by combined paraquat and iron and blocked paraquat-induced dopaminergic neuronal death. Furthermore, pretreatment with the synthetic superoxide dismutase/catalase mimetic, EUK-189, significantly decreased microglial activation mediated by combined paraquat and iron treatment. These findings support the notion that environmental PD risk factors may act synergetically to produce neurodegeneration associated with the disorder and that iron and paraquat may act via common oxidative stress-mediated mechanism involving microglial activation.

### Keywords

dopaminergic neurons; microglial activation; iron; oxidative; paraquat; Parkinsonism

### Introduction

Parkinson's disease (PD) is a progressive neurodegenerative disorder characterized by tremor, rigidity, bradykinesia, and postural instability. These clinical features are caused by the degeneration of dopaminergic neurons in the substantia nigra pars compacta (SNpc) region of the midbrain [1-3]. Although 5-10% of classical PD cases result from monogenetic mutations, the exact cause(s) of sporadic PD is unknown [1,4]. Epidemiological evidence suggests that late-onset idiopathic PD is not due to strict genetic inheritance [5]. This along with variations in incidence of PD by geographic region suggests that sporadic PD instead may be caused by exposure to environmental factors perhaps in concert with individual variations in genetic susceptibilities [6,7]. As PD is likely to be a multifactorial disorder, the use of *in vivo* models to explore the additive or synergistic effects of combined risk factors are likely to be of great importance in understanding sporadic disease etiology.

---

Address correspondence to: Julie K. Andersen, Buck Institute for Age Research, 8001 Redwood Blvd., Novato, CA 94945. Phone: (415) 209-2070; Fax: (415) 209-2231; Email: jandersen@buckinstitute.org.

**Publisher's Disclaimer:** This is a PDF file of an unedited manuscript that has been accepted for publication. As a service to our customers we are providing this early version of the manuscript. The manuscript will undergo copyediting, typesetting, and review of the resulting proof before it is published in its final citable form. Please note that during the production process errors may be discovered which could affect the content, and all legal disclaimers that apply to the journal pertain.

Exposure to either agricultural chemicals or metals have both widely been postulated as potential environmental risk factors for the disease and this is supported by extensive epidemiological evidence [7-13]. Pesticides, such as fumigants, fungicides, herbicides, insecticides, and rodenticides, represent one of the primary classes of environmental agents associated with PD [14,15]. Rotenone, a pesticide, causes highly selective nigrostriatal dopaminergic degeneration that is associated behaviorally with hypokinesia and rigidity [16]. Recently, we demonstrated that combined exposure to both neonatal iron and the widely used herbicide 1,1'-dimethyl-4,4'-bipyridium (paraquat, PQ) results in accelerated age-related neurodegeneration of midbrain dopaminergic neurons which can be prevented by antioxidant treatment [17]. This not only suggests that environmental agents may act synergistically to produce PD-related cell loss but that iron and paraquat in particular may act via a common oxidative stress mechanism.

Although the mechanism by which dopaminergic neurons degenerate in PD is still unknown, microglial-mediated neuroinflammation appears to play a critical role in disease pathogenesis [18-20]. Microglia activation is a hallmark of inflammation and is thought to contribute to the pathogenesis of PD by releasing cytotoxic agents such as pro-inflammatory cytokines and reactive oxygen species (ROS) that increase inflammation and oxidative stress. Degeneration of dopaminergic neurons in the human disorder is accompanied by massive microglial activation [21]. However, the molecular mechanisms by which paraquat induces microglial-mediated neuroinflammation are not yet fully understood. Here, we demonstrate that combined environmental exposure to paraquat and iron results in modulation in the microglial activation state. Apocynin, an NADPH oxidase inhibitor, was found in our study to attenuate the release of superoxide from microglia stimulated by combined paraquat and iron and block paraquat-induced dopaminergic neuronal death. Furthermore, pretreatment with the synthetic superoxide dismutase/catalase mimetic, EUK-189, significantly decreased microglial activation mediated by combined paraquat and iron treatment.

## Materials and Methods

### Materials

1,1'-dimethyl-4,4'-bipyridium dichloride (paraquat), carbonyl iron, and mouse anti-gial fibrillary acidic protein (GFAP) monoclonal antibody were purchased from Sigma (St. Louis, MO). Rat anti-mouse CD11b antibody was obtained from Serotec Inc. (Raleigh, NC). Sheep anti-tyrosine hydroxylase (TH) and mouse anti-neuron-specific nuclear protein (NeuN) antibodies were from Chemicon (Temecula, CA). Mouse anti-gp91phox antibody was purchased from BD Biosciences (San Jose, CA). Media and sera were obtained from Invitrogen. Osmotic minipumps (Alzet 2004) were from Alza Scientific Products (Mountain View, CA). The salen manganese complex EUK-189 was a gift from Proteome Systems, Inc. (Woburn, MA).

### Primary mesencephalic neuron-glia cultures

Primary mesencephalic neuron-glia cultures were prepared from embryonic gestation day 14-15 C57BL/6 mouse embryos as described previously [22-24]. Briefly, dissociated cells were seeded at  $7 \times 10^5$  cells per well onto poly-D-lysine-coated 24-well culture plates. Cultures were maintained at 37°C in a humidified atmosphere containing 95% air and 5% carbon dioxide, in minimum essential medium (MEM) containing 10% heat-inactivated fetal bovine serum (FBS), 10% heat-inactivated horse serum (HS), 1 g/L glucose, 2 mM glutamate, 1 mM sodium pyruvate, 100 µM nonessential amino acids, 100 units/ml penicillin, and 100 µg/ml streptomycin. After 4 days, one-half of the medium was replaced with fresh medium. Cells were grown an additional 3 days and then used for treatment. The cultures contained ~13%

CD11b-positive microglia, 47% GFAP-positive astrocytes, and 40% NeuN-positive neurons of which 4.2% were TH-positive neurons.

### Primary mesencephalic microglia cultures

Primary microglia cultures were prepared from postnatal day 1 C57BL/6 mice as described previously [22]. Briefly, whole brains were dissected, digested, and mechanically dissociated. Dissociated cells were seeded into poly-D-lysine-coated 175 cm<sup>2</sup> culture flasks. Cultures were maintained at 37°C in a humidified atmosphere containing 95% air and 5% CO<sub>2</sub>, in DMEM/F12 containing 10% FBS, 1 mM sodium pyruvate, 100 μM nonessential amino acids, 2 mM glutamate, 100 units/ml penicillin, and 100 μg/ml streptomycin. After 14 d, microglia were gently shaken off the cell cultures, collected by centrifugation, and seeded in poly-d-lysine-coated 96-well plates. This produced purified microglial cultures (≥ 95%), assessed by staining using antibodies against the microglial marker CD11b. After 1 d, microglia were rinsed twice and conditioned for 2 h in warm phenol red-free DMEM. Microglia were treated with vehicle or paraquat alone or plus FeCl<sub>2</sub>. To evaluate the effect of the salen manganese complex EUK-189, the compound was added 1 h prior to paraquat combined with iron. Treatment was performed at 37°C with 95% air and 5% CO<sub>2</sub> in a humidified environment.

### Primary mesencephalic neuron-enriched cultures

Mesencephalic neuron-enriched cultures were prepared from embryonic gestation day 14-15 C57BL/6 mouse embryos as described previously [22]. Briefly, dissociated cells were seeded at  $7 \times 10^5$  cells per well onto poly-D-lysine-coated 24-well culture plates. Cultures were maintained at 37°C in a humidified atmosphere containing 95% air and 5% carbon dioxide, in minimum essential medium (MEM) containing 10% FBS, 10% HS, 1 g/L glucose, 2 mM glutamate, 1 mM sodium pyruvate, 100 μM nonessential amino acids, 100 units/ml penicillin, and 100 μg/ml streptomycin. Two days later, the cultures were treated with 9 μM cytosine β-D-arabinofuranoside for 3 days to suppress the proliferation of glial cells and then were changed back to fresh medium. Seven-day-old cultures that contained <0.1% CD11b-positive microglia, <7.6% GFAP-positive astrocytes, and 92% NeuN-positive neurons of which 4.2% were TH-positive neurons were used for treatment.

### Measurement of superoxide production

The production of superoxide was determined by measuring the superoxide dismutase (SOD)-inhibitable reduction of the tetrazolium salt WST-1 [25,26]. Microglia-enriched cultures in 96-well culture plates were washed twice with HBSS without phenol red. Fifty microliters of HBSS with and without 600 U/ml SOD was added to each well along with 50 μl of WST-1 (1 mM) in HBSS, and 50 μl of vehicle, FeCl<sub>2</sub>, paraquat, or paraquat plus FeCl<sub>2</sub>. The absorbance at 450 nm was read with a SpectraMax 340 microplate spectrophotometer (Molecular Devices Corp, Sunnyvale, CA). The difference in absorbance observed in the presence and absence of SOD was considered to be the amount of superoxide produced. To evaluate the effect of the NADPH oxidase inhibitor apocynin or superoxide dismutase/catalase mimetic EUK-189 on superoxide release, these compounds were added 1 h prior to paraquat with or without FeCl<sub>2</sub>.

### Immunocytochemistry

Cultures were fixed with paraformaldehyde in phosphate-buffered saline and permeabilized with 0.3% Triton X-100 in phosphate-buffered saline as described previously [17,23,24]. Primary antibodies used in this study were mouse monoclonal anti-GFAP (1:500), rat polyclonal anti-CD11b (1:100), mouse monoclonal anti-gp91phox (1:100), mouse monoclonal anti-NeuN (1:500), and sheep polyclonal anti-TH (1:300). The secondary antibodies were rhodamine-conjugated donkey anti-mouse, or anti-sheep IgG (Jackson ImmunoResearch;

1:200) and fluorescein isothiocyanate-conjugated goat anti-rat IgG (Vector, Burlingame, CA, 1:200). 4',6-Diamidino-2-phenylindole (DAPI) (Vector) was used to counterstain nuclei. Control experiments were performed in which the primary antibody was omitted. No staining was observed under these conditions. Stained cells were counted in 10 randomly chosen microscopic fields (at least 500 cells). Data were expressed as the mean  $\pm$  SEM of the percentage of total cells that showed positive staining.

### Drug administration

C57BL/6 mice were obtained from the Jackson Laboratory (Bar Harbor, ME). Carbonyl iron was administered to male mice from postnatal days 10 to 17 via oral gavage at a dosage of 120 mg/kg. Control animals were fed equal volumes of sterile saline. Mice were aged to 2 and 12 months of age and were intraperitoneally injected with saline or 10 mg/kg paraquat twice per week for three weeks. Animals were killed at day 4 after final administration. Administration of the salen manganese complex EUK-189 was performed as previously described [17,24]. Briefly, mice were anesthetized with 4% isoflurane in 70% N<sub>2</sub>O/30% O<sub>2</sub> and subcutaneously implanted with an osmotic minipump containing either 5% mannitol (as vehicle control) or 15 mM EUK-189 (dissolved in 5% mannitol). Pumps delivered EUK-189 at a rate of 0.25  $\mu$ l/h for a 28-day period. Experimental protocols were in accordance with the National Institutes of Health Guidelines for Use of Live Animals and were approved by the Animal Care and Use Committee at the Buck Institute of Age Research.

### Immunohistochemistry

The accuracy of counting of double-labeled neurons was determined by analysis of systematically sampled candidate neurons from saline- or paraquat-treated brains. Sections were fixed with 4% paraformaldehyde in PBS, and incubated in blocking buffer (2% horse serum/0.2% Triton X-100/0.1% BSA in PBS) for 1 h at room temperature as described previously [17,23]. Primary antibodies used were sheep polyclonal anti-TH (1:500), mouse monoclonal anti-gp91<sup>phox</sup> (1:150), and rat polyclonal anti-CD11b (1:200). Primary antibodies were added in blocking buffer and incubated with sections at 4°C overnight. The secondary antibodies were Alexa Fluoro 488- or 594-conjugated donkey anti-sheep, anti-mouse, or anti-rat IgG (Molecular Probes; 1:200). Nuclei were counterstained with 4',6-diamidino-2-phenylindole (DAPI) using proLong Gold anti-fade reagent (Molecular Probes) and fluorescence signals were detected with an LSM 510 NLO Confocal Scanning System mounted on an Axiovert 200 inverted microscope (Carl Zeiss Ltd) equipped with a two-photon Chameleon laser (Coherent Inc.). Three-color images were scanned using Argon, 543 HeNe, and Chameleon (750-780 nm for DAPI) lasers. IMARIS (Bitplane AG) imaging software was used for three-dimensional image reconstruction. Images were acquired using LSM 510 Imaging Software (Carl Zeiss Ltd). The specificity of each label was first verified using single-channel scans that were then merged into multiple-channel views. Neurons were considered double-labeled if colabeling with relevant morphology was seen throughout the extent of the nucleus for nuclear markers or if a cytoplasmic marker surrounds a nuclear marker when viewed in  $x$ - $y$  cross-section as well as in  $x$ - $z$  and  $y$ - $z$  cross-sections produced by orthogonal reconstructions from  $z$ -stacks taken at 400x magnification. TH or CD11b single-labeled cells and cells double labeled for TH and gp91<sup>phox</sup> were recorded in three 50  $\mu$ m sections per animal. Controls included omitting or preabsorbing primary antibodies or omitting secondary antibodies [17,27].

### Statistical analysis

All data are expressed as mean  $\pm$  S.E.M. for the number ( $n$ ) of independent experiments performed. Differences among the means for all experiments described were analyzed using

two-way analysis of variance. Newman-Keuls post-hoc analysis was employed when differences were observed by analysis of variance testing ( $p < 0.05$ ).

## Results

### Dopaminergic cell death as a consequence of combined paraquat-iron-mediated toxicity requires the presence of glial cells

In order to assess the possible role of glial cells in dopaminergic cell death associated with combined paraquat/ $\text{FeCl}_2$  treatment, we assessed dopaminergic cell loss paraquat in primary mesencephalic neuron-glia or neuron-enriched cultures via immunofluorescence with antibody specific for tyrosine hydroxylase (TH). As shown in Figure 1, paraquat alone results in significant TH-positive neuronal cell death in primary mesencephalic neuron-glia but not neuronally enriched cultures. Dopaminergic cell loss is exacerbated in mixed cultures in the presence of  $\text{FeCl}_2$ ;  $\text{FeCl}_2$  treatment alone had no effect. These results suggest that paraquat-induced iron enhanced dopaminergic cell death requires the presence of glial cells.

### Microglial superoxide production is responsible for paraquat-mediated iron enhanced dopaminergic cell death *in vitro*

Since microglial activation-mediated oxidative stress has been previously implicated in other dopaminergic cell death paradigms (10-12), we chose to examine the potential role of microglia in neuronal loss following combined paraquat-iron neurotoxicity. We first treated primary microglia with combined paraquat and  $\text{FeCl}_2$  and measured extracellular superoxide production. As previously shown [28], paraquat alone was found to induce extracellular superoxide production by microglia in a dose-dependent manner (Figure 2A). Although exposure to  $5 \mu\text{M}$   $\text{FeCl}_2$  was nontoxic on its own,  $\text{FeCl}_2$  at this concentration significantly increased superoxide production induced by paraquat in a dose-dependent manner (Figure 2A). To test the time dependence of superoxide production stimulated by combined paraquat and  $\text{FeCl}_2$ , we treated microglia cultures with  $5 \mu\text{M}$   $\text{FeCl}_2$ ,  $1 \mu\text{M}$  paraquat, or  $1 \mu\text{M}$  paraquat plus  $5 \mu\text{M}$   $\text{FeCl}_2$  for 10-30 min. Although superoxide production in cultures treated with  $\text{FeCl}_2$  was not significant, a significant increase was observed in cultures treated with paraquat or paraquat plus  $\text{FeCl}_2$  as early as 10 min following treatment (Figure 2B). Pretreatment with the microglial NADPH inhibitor apocynin significantly inhibited paraquat-mediated iron-induced release of superoxide from microglia and subsequent TH-positive neuronal cell death (Figure 3). Apocynin alone at the concentrations used was neither stimulatory nor inhibitory in terms of neuronal survival (data not shown).

### Microglial activation itself is due to increased paraquat-mediated iron enhanced oxidative stress

The salen manganese complexes (EUKs), synthetic superoxide dismutase and catalase mimetics, have been shown to be neuroprotective in several animal models including systemic paraquat exposure [17,24,29-32]. To test whether EUK-189 was protective against exacerbated neuroinflammation induced by paraquat combined with  $\text{FeCl}_2$ , primary microglia cultures were pretreated with  $25 \mu\text{M}$  EUK-189 1 h prior to treatment with combined paraquat- $\text{FeCl}_2$ . The numbers of gp91<sup>phox</sup>-positive cells (indicative of microglial NADPH oxidase activation) at 1 h and superoxide production at 20 min were measured. As demonstrated in Figure 4A and B, EUK-189 significantly reduced the numbers of gp91<sup>phox</sup>-positive cells and superoxide production to the same level in the presence of paraquat alone or paraquat and iron combined. Furthermore, neutralization of superoxide by EUK-189 increased the number of TH-positive neurons in primary mesencephalic neuron-glia cultures treated with paraquat alone or paraquat and iron combined to nearly control culture levels (Figure 4C). EUK-189 alone at the concentrations used was neither stimulatory nor inhibitory in terms of neuronal survival (data not shown).

## EUK-189 prevents microglia activation elicited by combined iron and paraquat exposure *in vivo*

Systemic administration of paraquat in young (2 month old) mice was previously reported to increase levels of gp91<sup>phox</sup> in the SNpc [33]. In order to determine whether additional loss of SNpc neurons elicited by combined paraquat-iron exposure is due to increased microglial activation and subsequent increases in levels of oxidative stress, pups were first fed iron daily from postnatal days 10-17 as previously described [17,34]. They were housed with their mothers until weaning at week three and aged to either 2 or 12 months of age. At the end of each time period, a subset of iron vs. vehicle-fed mice were intraperitoneally injected with saline or paraquat as previously described [17,35] and sacrificed at day 5. No signs of acute systemic toxicity were observed in the iron-fed pups at the dosages used in this study [34]. No changes in body weights were observed in the mice at the dosage of paraquat used in the experiments [35]. We performed immunofluorescent double-labeling experiments using CD11b as a microglia marker and gp91<sup>phox</sup> as a biomarker for NADPH oxidase. Neonatal iron alone does not result in increased levels of NADPH oxidase within SNpc microglia at 2 months of age, but by 12 months of age there is a significant increase in this parameter, although we previously demonstrated that this is not associated with an increase in dopaminergic cell loss in this brain region [17,34]. As previously demonstrated, paraquat administration at 2 months results in increases in gp91<sup>phox</sup> levels [33] that are further increased by 12 months of age and are exacerbated in the presence of neonatal iron exposure (Figure 5).

To investigate whether EUK-189 inhibited the increased gp91<sup>phox</sup> level in the SNpc following paraquat administration in the 2- or 12-month-old iron-fed mice versus those treated with paraquat alone, we implanted mice with osmotic minipumps containing either 5% mannitol (as vehicle control) or 15 mM EUK-189 3 days prior to paraquat treatment [17,24,36]. As shown in Figure 4, pretreatment with EUK-189 was found to attenuate the age-related increases in gp91<sup>phox</sup>-positive microglia induced not only by either agent alone but also as a consequence of combined iron and paraquat exposure where an increase in dopaminergic SNpc cell loss occurs [17].

We next examined the expression of CD11b, a specific marker for activated microglia. As shown in Figure 6A, CD11b immunoreactivity was minimal within the SNpc of control mice. However, robust microglia (CD11b-positive) activation was evident within the SNpc of paraquat-treated mice. Morphologically, CD11b-positive cells appeared more compact, rounded, and with obvious cellular thickening, indicative of an activated state [37], when compared with saline-treated control mice that displayed a more ramified appearance with thin processes. Furthermore, quantification of activated microglial has found to be elevated within the SNpc of paraquat-treated animals previously fed iron versus those controls previously fed only saline (Figure 6B). Moreover, EUK-189 administration reduced the number of activated microglial within the SNpc to a similar extent in animals treated with paraquat alone or in combination with iron (Figure 6B). Taken together, our data demonstrate that EUK-189 attenuates both the exacerbation in paraquat-elicited microglial activation induced by neonatal iron feeding as well as age-related increases in nigrostriatal dopaminergic cell death [17].

## Discussion

In this study, we show that iron-enhanced paraquat-induced dopaminergic cell death was mediated through the presence of microglia and the activation of NADPH oxidase, which resulted in the production of the extracellular reactive oxygen species (ROS) responsible for dopaminergic neurotoxicity. We have not ruled out a role for astrocytes in the neurotoxic effects. Our data clearly shows, however, the involvement of microglia. Under physiological conditions, microglia play an important role in immune surveillance. In response to immunological challenges such as invading pathogens and neuronal injuries, microglia become

activated displaying a plastic amoeboid morphology [38]. Degeneration of dopaminergic neurons in Parkinson's disease is accompanied by massive microglial activity and accumulation of proinflammatory cytokines [21]. Microglial activation has been noted postmortem in both humans and primates exposed to MPTP [39,40]. Several murine models of the disorder including systemic acute 1-methyl-4-phenyl-1,2,3,6-tetrahydropyridine (MPTP) [41-43], chronic rotenone administration [44] and intrastriatal 6-hydroxydopamine (6-OHDA) infusion [45] also exhibit increased levels of microglial activation similar to what is found in PD. In addition, lipopolysaccharide (LPS) mediates microglial activation and subsequently the degeneration of nigrostriatal dopaminergic neurons both *in vitro* and *in vivo* [46-48]. In the rotenone model, microglial activation has been detected before the appearance of a dopaminergic lesion [44]. Aggregated  $\alpha$ -synuclein, the major component of Lewy bodies in patients with PD or dementia with Lewy bodies (DLB), can activate microglia and enhance  $\alpha$ -synuclein-mediated dopaminergic neurotoxicity. Microglial phagocytosis of  $\alpha$ -synuclein appears to be pivotal in aggregated  $\alpha$ -synuclein-induced microglial neurotoxicity [49]. Systemic exposure to proteasome inhibitors (epoxomicin and PSI) have also been shown to cause a concomitant appearance of Lewy bodies containing aggregated  $\alpha$ -synuclein and microglia activation in the SNpc although this model has been recently questioned [50].

Oxidant-induced iron signaling and the subsequent occurrence of free radical-mediated oxidative damage are becoming increasingly understood as playing highly significant roles in neurodegeneration [51]. Elevated SN iron levels have also been reported to be associated with sporadic PD [52-55]. Redox-available iron has been detected in Lewy bodies within SNpc of postmortem parkinsonian brains [56] and the oxidation state of iron has been found to change from ferrous to ferric ion in SNpc dopaminergic neurons during PD progression [57]. This alteration in redox state has been postulated to be due to iron's capacity to catalyze oxidative reactions. The high concentration of iron within the SN may act to catalyze the conversion of  $H_2O_2$  produced during breakdown of dopamine to highly reactive hydroxyl radicals resulting in increased oxidative damage in the region [53]. We recently demonstrated that older iron-fed animals are more susceptible to exposure to the herbicide paraquat than younger iron-fed animals and that paraquat administration accelerates SN dopaminergic cell loss in these animals as a consequence of this early exposure to iron [17].

Paraquat administration at the same or similar dosage regimes used in this current study have previously been shown not only to cross the blood-brain-barrier (BBB) through the neutral amino acid transporter [58] but also to selectively damage the nigrostriatal dopaminergic system in mice [23,24,59]. The mechanism of paraquat neurotoxicity appears to be mediated via oxidative stress. Superoxide anion radicals are generated by paraquat through both redox cycling via reaction with molecular oxygen and electron transfer reactions with NADH-dependent oxidoreductases [60-62]. We previously reported evidence that suggests paraquat mediates dopaminergic cell death via oxidative stress-mediated activation of the JNK signaling pathway [17,23,24].

The NADPH oxidase consists of membrane-bound subunits, gp91<sup>phox</sup> and p22<sup>phox</sup>, which constitute the flavocytochrome b558 complex, and cytosolic subunits p40<sup>phox</sup>, p47<sup>phox</sup>, p67<sup>phox</sup>, and the small G-protein Rac. Activation of the NADPH oxidase occurs when the microglial cell is exposed to injury or immunological challenges initiating the activation of multiple parallel intracellular signaling cascades. The assembly of a fully functional NADPH oxidase catalyzes the transfer of electrons from NADPH to molecular oxygen, resulting in the generation of superoxide. Our studies with the microglial NADPH oxidase inhibitor, apocynin, or microglia-depleted cultures have shown that NADPH oxidase-derived superoxide might be a major factor in mediating the microglia-enhanced combined paraquat and iron neurotoxicity. In NADPH-oxidase null mice (gp91<sup>phox</sup> <sup>-/-</sup>) sequential paraquat injections failed to cause any significant loss of nigral dopaminergic neurons *in vitro* [28] or *in vivo* [33]. Taken together,

these data suggest that microglial NADPH oxidase renders dopaminergic neurons more sensitive to paraquat neurotoxicity.

The salen manganese EUK complexes catalytically eliminate both superoxide and hydrogen peroxide [29,63,64] and have been shown to be neuroprotective in several animal models of PD [17,24,65]. The EUK-189 compound used in this study is more lipophilic than earlier generations of salen-manganese complexes thus improving intracellular and intra-organellar delivery [66]. While we have not ruled out that EUK acts by peripherally impacting on entry of paraquat and/or iron into the brain, EUK compounds have been demonstrated to ameliorate brain-specific injury in several in vivo model systems indicating its ability to cross the blood-brain-barrier and elicit protective antioxidant effects [29,66-68]. The present findings support a pre-eminent role for oxidative stress in neurodegeneration and impairment of dopaminergic function in an experimental model of PD involving combined environmental exposure and suggest that inhibition of ROS production from microglia may provide improved prevention and treatment for Parkinson's disease and other neurodegenerative disorders.

## Acknowledgements

This work was supported by National Institutes of Health Grant U54 ES12077 (JKA).

## References

1. Dauer W, Przedborski S. Parkinson's disease: mechanisms and models. *Neuron* 2003;39:889–909. [PubMed: 12971891]
2. Forno LS. Neuropathology of Parkinson's disease. *J Neuropathol Exp Neurol* 1996;55:259–272. [PubMed: 8786384]
3. Lang AE, Lozano AM. Parkinson's disease. First of two parts. *N Engl J Med* 1998;339:1044–1053. [PubMed: 9761807]
4. Olanow CW, Tatton WG. Etiology and pathogenesis of Parkinson's disease. *Annu Rev Neurosci* 1999;22:123–144. [PubMed: 10202534]
5. Tanner CM, Ottman R, Goldman SM, Ellenberg J, Chan P, Mayeux R, Langston JW. Parkinson disease in twins: an etiologic study. *JAMA* 1999;281:341–346. [PubMed: 9929087]
6. Lanska DJ. The geographic distribution of Parkinson's disease mortality in the United States. *J Neurol Sci* 1997;150:63–70. [PubMed: 9260859]
7. Liou HH, Tsai MC, Chen CJ, Jeng JS, Chang YC, Chen SY, Chen RC. Environmental risk factors and Parkinson's disease: a case-control study in Taiwan. *Neurology* 1997;48:1583–1588. [PubMed: 9191770]
8. Gorell JM, Johnson CC, Rybicki BA, Peterson EL, Richardson RJ. The risk of Parkinson's disease with exposure to pesticides, farming, well water, and rural living. *Neurology* 1998;50:1346–1350. [PubMed: 9595985]
9. Hertzman C, Wiens M, Bowering D, Snow B, Calne D. Parkinson's disease: a case-control study of occupational and environmental risk factors. *Am J Ind Med* 1990;17:349–355. [PubMed: 2305814]
10. Hubble JP, Cao T, Hassanein RE, Neuberger JS, Koller WC. Risk factors for Parkinson's disease. *Neurology* 1993;43:1693–1697. [PubMed: 8414014]
11. Jimenez-Jimenez FJ, Mateo D, Gimenez-Roldan S. Exposure to well water and pesticides in Parkinson's disease: a case-control study in the Madrid area. *Mov Disord* 1992;7:149–152. [PubMed: 1584237]
12. Semchuk KM, Love EJ, Lee RG. Parkinson's disease and exposure to agricultural work and pesticide chemicals. *Neurology* 1992;42:1328–1335. [PubMed: 1620342]
13. Stephenson J. Exposure to home pesticides linked to Parkinson disease. *JAMA* 2000;283:3055–3056. [PubMed: 10865282]
14. Hatcher JM, Pennell KD, Miller GW. Parkinson's disease and pesticides: a toxicological perspective. *Trends Pharmacol Sci* 2008;29:322–329. [PubMed: 18453001]



15. Dick FD. Parkinson's disease and pesticide exposures. *Br Med Bull* 2006;79-80:219–231. [PubMed: 17242039]
16. Betarbet R, Sherer TB, MacKenzie G, Garcia-Osuna M, Panov AV, Greenamyre JT. Chronic systemic pesticide exposure reproduces features of Parkinson's disease. *Nat Neurosci* 2000;3:1301–1306. [PubMed: 11100151]
17. Peng J, Peng L, Stevenson FF, Doctrow SR, Andersen JK. Iron and paraquat as synergistic environmental risk factors in sporadic Parkinson's disease accelerate age-related neurodegeneration. *J Neurosci* 2007;27:6914–6922. [PubMed: 17596439]
18. Hunot S, Hirsch EC. Neuroinflammatory processes in Parkinson's disease. *Ann Neurol* 2003;53 (Suppl 3):S49–58. [PubMed: 12666098]discussion S58-60
19. Wersinger C, Sidhu A. An inflammatory pathomechanism for Parkinson's disease? *Curr Med Chem* 2006;13:591–602. [PubMed: 16515523]
20. Wyss-Coray T, Mucke L. Inflammation in neurodegenerative disease--a double-edged sword. *Neuron* 2002;35:419–432. [PubMed: 12165466]
21. McGeer PL, Itagaki S, Boyes BE, McGeer EG. Reactive microglia are positive for HLA-DR in the substantia nigra of Parkinson's and Alzheimer's disease brains. *Neurology* 1988;38:1285–1291. [PubMed: 3399080]
22. Gao HM, Liu B, Hong JS. Critical role for microglial NADPH oxidase in rotenone-induced degeneration of dopaminergic neurons. *J Neurosci* 2003;23:6181–6187. [PubMed: 12867501]
23. Peng J, Mao XO, Stevenson FF, Hsu M, Andersen JK. The herbicide paraquat induces dopaminergic nigral apoptosis through sustained activation of the JNK pathway. *J Biol Chem* 2004;279:32626–32632. [PubMed: 15155744]
24. Peng J, Stevenson FF, Doctrow SR, Andersen JK. Superoxide dismutase/catalase mimetics are neuroprotective against selective paraquat-mediated dopaminergic neuron death in the substantia nigra: implications for Parkinson disease. *J Biol Chem* 2005;280:29194–29198. [PubMed: 15946937]
25. Peskin AV, Winterbourn CC. A microtiter plate assay for superoxide dismutase using a water-soluble tetrazolium salt (WST-1). *Clin Chim Acta* 2000;293:157–166. [PubMed: 10699430]
26. Tan AS, Berridge MV. Superoxide produced by activated neutrophils efficiently reduces the tetrazolium salt, WST-1 to produce a soluble formazan: a simple colorimetric assay for measuring respiratory burst activation and for screening anti-inflammatory agents. *J Immunol Methods* 2000;238:59–68. [PubMed: 10758236]
27. Peng J, Xie L, Stevenson FF, Melov S, Di Monte DA, Andersen JK. Nigrostriatal dopaminergic neurodegeneration in the weaver mouse is mediated via neuroinflammation and alleviated by minocycline administration. *J Neurosci* 2006;26:11644–11651. [PubMed: 17093086]
28. Wu XF, Block ML, Zhang W, Qin L, Wilson B, Zhang WQ, Veronesi B, Hong JS. The role of microglia in paraquat-induced dopaminergic neurotoxicity. *Antioxid Redox Signal* 2005;7:654–661. [PubMed: 15890010]
29. Baker K, Marcus CB, Huffman K, Kruk H, Malfroy B, Doctrow SR, Gonzalez PK, Zhuang J, Benson PF, Menconi MJ, Fink MP, Baudry M, Etienne S, Bruce A, Palucki M, Jacobsen E. Synthetic combined superoxide dismutase/catalase mimetics are protective as a delayed treatment in a rat stroke model: a key role for reactive oxygen species in ischemic brain injury. *J Pharmacol Exp Ther* 1998;284:215–221. [PubMed: 9435181]
30. Jung C, Rong Y, Doctrow S, Baudry M, Malfroy B, Xu Z. Synthetic superoxide dismutase/catalase mimetics reduce oxidative stress and prolong survival in a mouse amyotrophic lateral sclerosis model. *Neurosci Lett* 2001;304:157–160. [PubMed: 11343826]
31. Malfroy B, Doctrow SR, Orr PL, Tocco G, Fedoseyeva EV, Benichou G. Prevention and suppression of autoimmune encephalomyelitis by EUK-8, a synthetic catalytic scavenger of oxygen-reactive metabolites. *Cell Immunol* 1997;177:62–68. [PubMed: 9140096]
32. Rong Y, Doctrow SR, Tocco G, Baudry M. EUK-134, a synthetic superoxide dismutase and catalase mimetic, prevents oxidative stress and attenuates kainate-induced neuropathology. *Proc Natl Acad Sci U S A* 1999;96:9897–9902. [PubMed: 10449791]

33. Purisai MG, McCormack AL, Cumine S, Li J, Isla MZ, Di Monte DA. Microglial activation as a priming event leading to paraquat-induced dopaminergic cell degeneration. *Neurobiol Dis* 2007;25:392–400. [PubMed: 17166727]
34. Kaur D, Peng J, Chinta SJ, Rajagopalan S, Di Monte DA, Cherny RA, Andersen JK. Increased murine neonatal iron intake results in Parkinson-like neurodegeneration with age. *Neurobiol Aging* 2007;28:907–913. [PubMed: 16765489]
35. Thiruchelvam M, McCormack A, Richfield EK, Baggs RB, Tank AW, Di Monte DA, Cory-Slechta DA. Age-related irreversible progressive nigrostriatal dopaminergic neurotoxicity in the paraquat and maneb model of the Parkinson's disease phenotype. *Eur J Neurosci* 2003;18:589–600. [PubMed: 12911755]
36. Zhang HJ, Doctrow SR, Xu L, Oberley LW, Beecher B, Morrison J, Oberley TD, Kregel KC. Redox modulation of the liver with chronic antioxidant enzyme mimetic treatment prevents age-related oxidative damage associated with environmental stress. *FASEB J* 2004;18:1547–1549. [PubMed: 15319374]
37. Soltys Z, Ziaja M, Pawlinski R, Setkowicz Z, Janeczko K. Morphology of reactive microglia in the injured cerebral cortex. Fractal analysis and complementary quantitative methods. *J Neurosci Res* 2001;63:90–97. [PubMed: 11169618]
38. Kreutzberg GW. Microglia: a sensor for pathological events in the CNS. *Trends Neurosci* 1996;19:312–318. [PubMed: 8843599]
39. Langston JW, Forno LS, Tetrud J, Reeves AG, Kaplan JA, Karluk D. Evidence of active nerve cell degeneration in the substantia nigra of humans years after 1-methyl-4-phenyl-1,2,3,6-tetrahydropyridine exposure. *Ann Neurol* 1999;46:598–605. [PubMed: 10514096]
40. McGeer PL, Schwab C, Parent A, Doudet D. Presence of reactive microglia in monkey substantia nigra years after 1-methyl-4-phenyl-1,2,3,6-tetrahydropyridine administration. *Ann Neurol* 2003;54:599–604. [PubMed: 14595649]
41. Wu DC, Jackson-Lewis V, Vila M, Tieu K, Teismann P, Vadseth C, Choi DK, Ischiropoulos H, Przedborski S. Blockade of microglial activation is neuroprotective in the 1-methyl-4-phenyl-1,2,3,6-tetrahydropyridine mouse model of Parkinson disease. *J Neurosci* 2002;22:1763–1771. [PubMed: 11880505]
42. Du Y, Ma Z, Lin S, Dodel RC, Gao F, Bales KR, Triarhou LC, Chernet E, Perry KW, Nelson DL, Luecke S, Phebus LA, Bymaster FP, Paul SM. Minocycline prevents nigrostriatal dopaminergic neurodegeneration in the MPTP model of Parkinson's disease. *Proc Natl Acad Sci U S A* 2001;98:14669–14674. [PubMed: 11724929]
43. Kurkowska-Jastrzebska I, Wronska A, Kohutnicka M, Czlonkowski A, Czlonkowska A. The inflammatory reaction following 1-methyl-4-phenyl-1,2,3, 6-tetrahydropyridine intoxication in mouse. *Exp Neurol* 1999;156:50–61. [PubMed: 10192776]
44. Sherer TB, Betarbet R, Kim JH, Greenamyre JT. Selective microglial activation in the rat rotenone model of Parkinson's disease. *Neurosci Lett* 2003;341:87–90. [PubMed: 12686372]
45. He Y, Appel S, Le W. Minocycline inhibits microglial activation and protects nigral cells after 6-hydroxydopamine injection into mouse striatum. *Brain Res* 2001;909:187–193. [PubMed: 11478935]
46. Gao HM, Jiang J, Wilson B, Zhang W, Hong JS, Liu B. Microglial activation-mediated delayed and progressive degeneration of rat nigral dopaminergic neurons: relevance to Parkinson's disease. *J Neurochem* 2002;81:1285–1297. [PubMed: 12068076]
47. Taylor DL, Diemel LT, Pocock JM. Activation of microglial group III metabotropic glutamate receptors protects neurons against microglial neurotoxicity. *J Neurosci* 2003;23:2150–2160. [PubMed: 12657674]
48. Castano A, Herrera AJ, Cano J, Machado A. Lipopolysaccharide intranigral injection induces inflammatory reaction and damage in nigrostriatal dopaminergic system. *J Neurochem* 1998;70:1584–1592. [PubMed: 9580157]
49. Zhang W, Wang T, Pei Z, Miller DS, Wu X, Block ML, Wilson B, Zhang W, Zhou Y, Hong JS, Zhang J. Aggregated alpha-synuclein activates microglia: a process leading to disease progression in Parkinson's disease. *FASEB J* 2005;19:533–542. [PubMed: 15791003]

50. McNaught KS, Perl DP, Brownell AL, Olanow CW. Systemic exposure to proteasome inhibitors causes a progressive model of Parkinson's disease. *Ann Neurol* 2004;56:149–162. [PubMed: 15236415]
51. Drechsel DA, Patel M. Role of reactive oxygen species in the neurotoxicity of environmental agents implicated in Parkinson's disease. *Free Radic Biol Med* 2008;44:1873–1886. [PubMed: 18342017]
52. Griffiths PD, Dobson BR, Jones GR, Clarke DT. Iron in the basal ganglia in Parkinson's disease. An in vitro study using extended X-ray absorption fine structure and cryoelectron microscopy. *Brain* 1999;122:667–673. [PubMed: 10219780]
53. Jellinger KA, Kienzl E, Rumpelmaier G, Paulus W, Riederer P, Stachelberger H, Youdim MB, Ben-Shachar D. Iron and ferritin in substantia nigra in Parkinson's disease. *Adv Neurol* 1993;60:267–272. [PubMed: 8420142]
54. Riederer P, Durr A, Goetz M, Sofic E, Jellinger K, Youdim MB. Distribution of iron in different brain regions and subcellular compartments in Parkinson's disease. *Ann Neurol* 1992;32:S101–104. [PubMed: 1510366]
55. Sofic E, Paulus W, Jellinger K, Riederer P, Youdim MB. Selective increase of iron in substantia nigra zona compacta of parkinsonian brains. *J Neurochem* 1991;56:978–982. [PubMed: 1704426]
56. Castellani RJ, Siedlak SL, Perry G, Smith MA. Sequestration of iron by Lewy bodies in Parkinson's disease. *Acta Neuropathol (Berl)* 2000;100:111–114. [PubMed: 10963356]
57. Yoshida S, Ektessabi A, Fujisawa S. XANES spectroscopy of a single neuron from a patient with Parkinson's disease. *J Synchrotron Radiat* 2001;8:998–1000. [PubMed: 11513007]
58. McCormack AL, Di Monte DA. Effects of L-dopa and other amino acids against paraquat-induced nigrostriatal degeneration. *J Neurochem* 2003;85:82–86. [PubMed: 12641729]
59. McCormack AL, Thiruchelvam M, Manning-Bog AB, Thiffault C, Langston JW, Cory-Slechta DA, Di Monte DA. Environmental risk factors and Parkinson's disease: selective degeneration of nigral dopaminergic neurons caused by the herbicide paraquat. *Neurobiol Dis* 2002;10:119–127. [PubMed: 12127150]
60. Burkitt MJ, Kadiiska MB, Hanna PM, Jordan SJ, Mason RP. Electron spin resonance spin-trapping investigation into the effects of paraquat and desferrioxamine on hydroxyl radical generation during acute iron poisoning. *Mol Pharmacol* 1993;43:257–263. [PubMed: 8381512]
61. Bus JS, Gibson JE. Paraquat: model for oxidant-initiated toxicity. *Environ Health Perspect* 1984;55:37–46. [PubMed: 6329674]
62. Clejan L, Cederbaum AI. Synergistic interactions between NADPH-cytochrome P-450 reductase, paraquat, and iron in the generation of active oxygen radicals. *Biochem Pharmacol* 1989;38:1779–1786. [PubMed: 2500125]
63. Baudry M, Etienne S, Bruce A, Palucki M, Jacobsen E, Malfroy B. Salen-manganese complexes are superoxide dismutase-mimics. *Biochem Biophys Res Commun* 1993;192:964–968. [PubMed: 8484797]
64. Gonzalez PK, Zhuang J, Doctrow SR, Malfroy B, Benson PF, Menconi MJ, Fink MP, Baudry M, Etienne S, Bruce A, Palucki M, Jacobsen E. EUK-8, a synthetic superoxide dismutase and catalase mimetic, ameliorates acute lung injury in endotoxemic swine. *J Pharmacol Exp Ther* 1995;275:798–806. [PubMed: 7473169]
65. Doctrow SR, Huffman K, Marcus CB, Musleh W, Bruce A, Baudry M, Malfroy B. Salen-manganese complexes: combined superoxide dismutase/catalase mimics with broad pharmacological efficacy. *Adv Pharmacol* 1997;38:247–269. [PubMed: 8895812]
66. Melov S, Doctrow SR, Schneider JA, Haberson J, Patel M, Coskun PE, Huffman K, Wallace DC, Malfroy B. Lifespan extension and rescue of spongiform encephalopathy in superoxide dismutase 2 nullizygous mice treated with superoxide dismutase-catalase mimetics. *J Neurosci* 2001;21:8348–8353. [PubMed: 11606622]
67. Browne SE, Roberts LJ 2nd, Dennery PA, Doctrow SR, Beal MF, Barlow C, Levine RL. Treatment with a catalytic antioxidant corrects the neurobehavioral defect in ataxia-telangiectasia mice. *Free Radic Biol Med* 2004;36:938–942. [PubMed: 15019978]
68. Liu R, Liu IY, Bi X, Thompson RF, Doctrow SR, Malfroy B, Baudry M. Reversal of age-related learning deficits and brain oxidative stress in mice with superoxide dismutase/catalase mimetics. *Proc Natl Acad Sci U S A* 2003;100:8526–8531. [PubMed: 12815103]

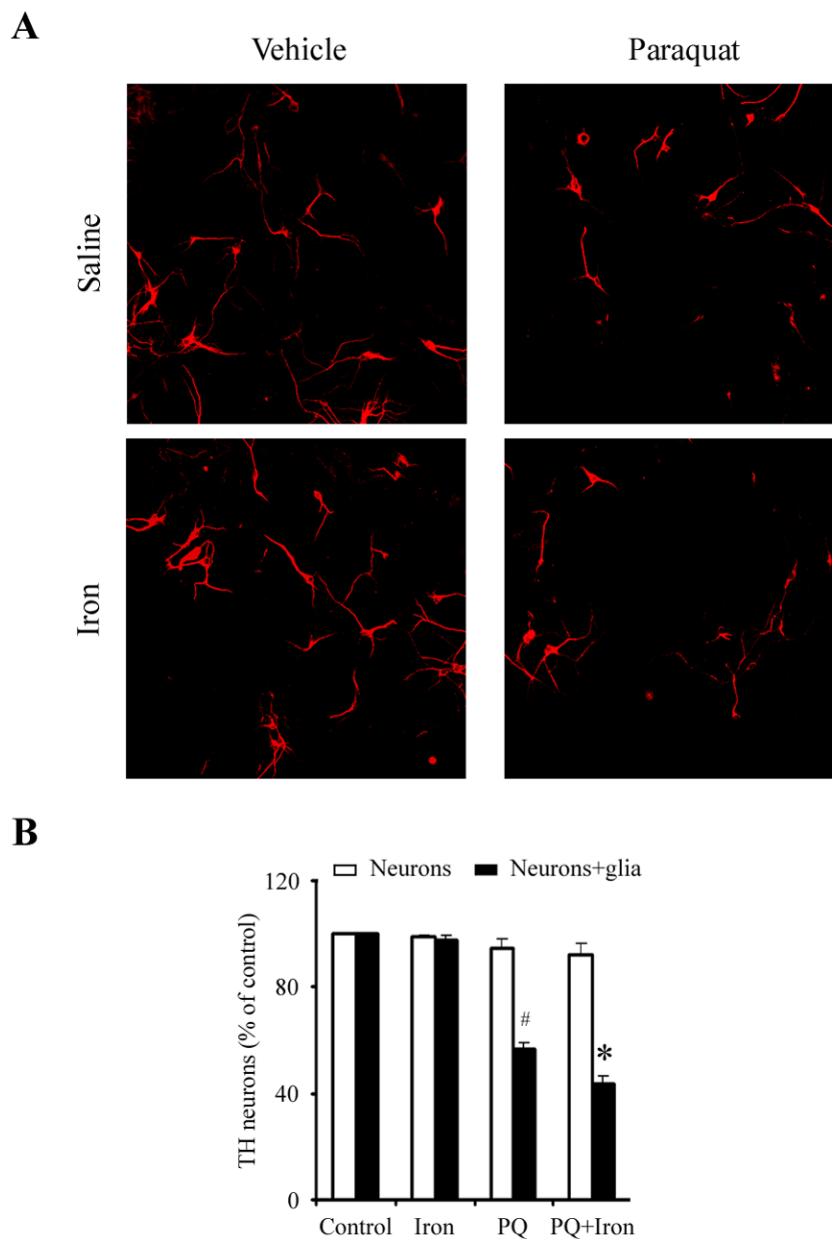


**Figure 1. Iron enhances paraquat-stimulated neurodegeneration requires glial cells**  
 (A) Photomicrographs of TH-positive neurons (red) in primary mesencephalic neuron-glia cultures. (B) Microglia enhanced dopaminergic neurodegeneration induced by combined iron and paraquat. Primary mesencephalic cultures were treated for 5 d with vehicle, 5  $\mu\text{M}$   $\text{FeCl}_2$ , 1  $\mu\text{M}$  paraquat, or 1  $\mu\text{M}$  paraquat plus 5  $\mu\text{M}$   $\text{FeCl}_2$ . #,  $p < 0.01$ , significantly from control; \*,  $p < 0.05$ , significantly from paraquat alone. Mean  $\pm$  S.E.M.,  $n = 4$ .

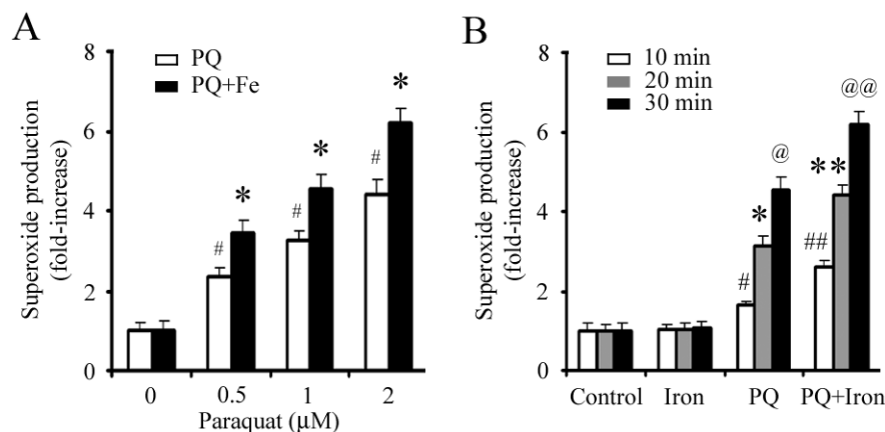


**Figure 2. Iron increases paraquat-stimulated microglial superoxide production *in vitro***  
 (A) Microglia were treated with increasing concentrations of paraquat and 5 μM FeCl<sub>2</sub> for 20 min. #, *p* < 0.01, significantly from control; \*, *p* < 0.01, significantly from paraquat alone. (B) Time course of paraquat-stimulated superoxide production. Microglia were treated with 5 μM FeCl<sub>2</sub>, 1 μM paraquat, or 1 μM paraquat plus 5 μM FeCl<sub>2</sub> for different time. #, *p* < 0.05; \*, *p* < 0.01; @ *p* < 0.001, compared to the time-matched control. ##, *p* < 0.05; \*\*, *p* < 0.05; @@ *p* < 0.01, compared to the time-matched paraquat alone. Mean ± S.E.M., n = 4.

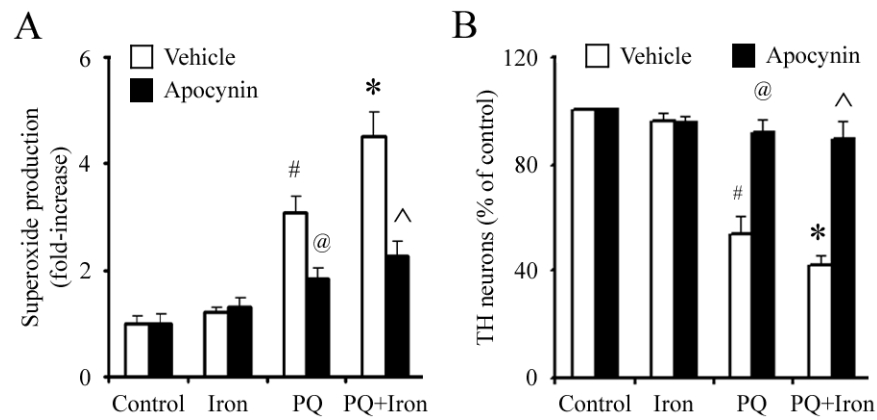


**Figure 3. The microglial NADPH oxidase inhibitor apocynin protects against dopaminergic neurons against combined paraquat-iron neurotoxicity *in vitro***

(A) Paraquat-stimulated release of superoxide in microglia. (B) TH-positive neuron counts in primary mesencephalic neuron-glia cultures. Mean  $\pm$  S.E.M., n = 4-5. #,  $p < 0.01$ , significantly from control plus vehicle group; \*,  $p < 0.05$ , significantly from paraquat plus vehicle group; @,  $p < 0.001$ , significantly from paraquat plus vehicle group; ^,  $p < 0.001$ , significantly from paraquat plus iron plus vehicle group.

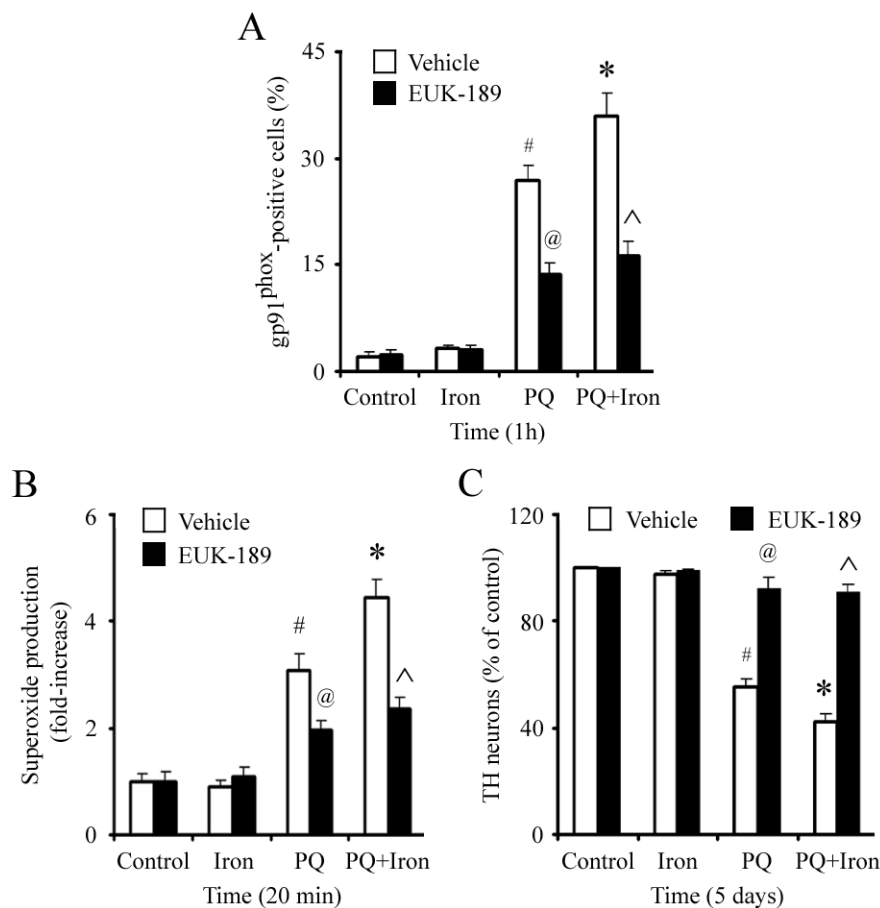


**Figure 4. EUK-189 suppresses paraquat-iron neurotoxicity by inhibition of microglia activation and subsequent NADPH oxidase-induced oxidative stress *in vitro***  
 (A) Gp91<sup>phox</sup>-positive microglia in primary microglia cultures. (B) Paraquat-stimulated release of superoxide in microglia. (C) TH-positive neuron counts in primary mesencephalic neuron-glia cultures. Mean ± S.E.M., n = 4-5. #, *p* < 0.01, significantly from control plus vehicle group; \*, *p* < 0.05, significantly from paraquat plus vehicle group; @, *p* < 0.001, significantly from paraquat plus vehicle group; ^, *p* < 0.001, significantly from paraquat plus iron plus vehicle group.

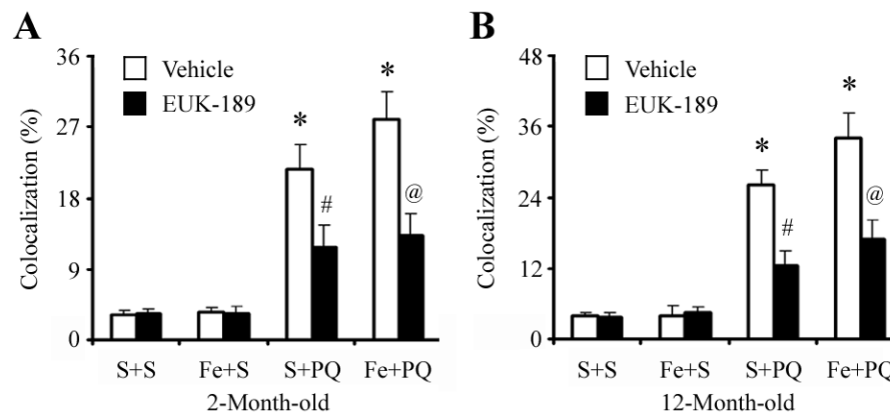


**Figure 5. Administration of EUK-189 attenuates combined neonatal paraquat-iron-induced microglial NADPH oxidase activation in the SNpc**

Quantitative analysis of double labeling for activated microglia with gp91<sup>phox</sup> in the SNpc of 2-month-old (A) and 12-month-old (B) mice. Mean  $\pm$  S.E.M., n = 3. \*,  $p < 0.001$ , significantly from saline plus saline plus vehicle group; #,  $p < 0.001$ , significantly from saline plus paraquat plus vehicle group; @,  $p < 0.001$ , significantly from neonatal iron fed plus paraquat plus vehicle group.



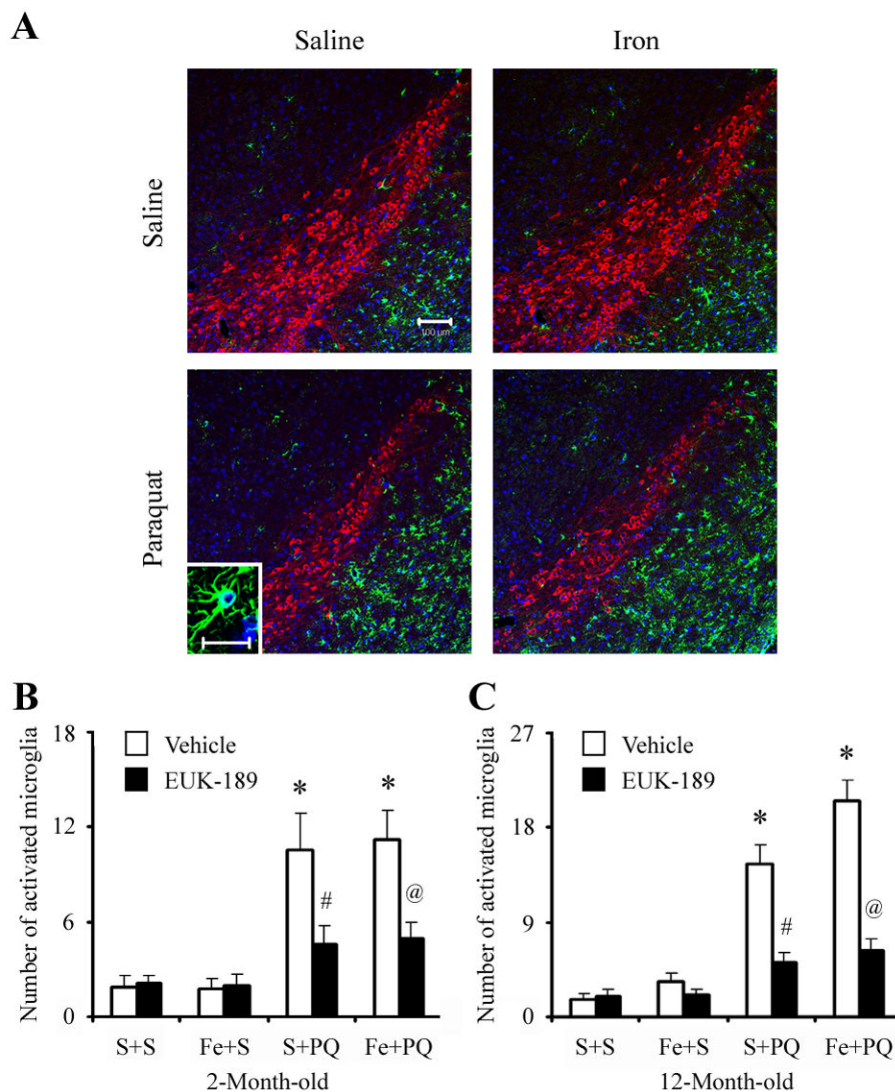


**Figure 6. Administration of EUK-189 inhibits microglial activation elicited by combined paraquat-iron versus paraquat alone in the SNpc**

(A) CD11b-positive microglia (green) localized within TH-positive SNpc neurons (red). 4',6-Diamidino-2-phenylindole (blue) was used to counterstain nuclei. Scale bar, 100  $\mu$ m. Insert image is a photomicrograph of representative activated microglial cell in the SNpc. Scale bar, 20  $\mu$ m. Quantitative analysis of the number of activated microglia in the SNpc of 2-month-old (B) and 12-month-old (C) mice. Mean  $\pm$  S.E.M., n = 3. \*,  $p < 0.001$ , significantly from saline plus saline plus vehicle group; #,  $p < 0.001$ , significantly from saline plus paraquat plus vehicle group; @,  $p < 0.001$ , significantly from neonatal iron fed plus paraquat plus vehicle group.